α formation probability in ^{10}Be and ^{12}Be within a microscopic cluster model

Qing Zhao,[1,*] Masaaki Kimura,[2,3,4] Bo Zhou,[5] and Seung-heon Shin[3]

[1]*School of Science, Huzhou University, Huzhou 313000, Zhejiang, China*
[2]*Nuclear Reaction Data Centre (JCPRG), Hokkaido University, Sapporo 060-0810, Japan*
[3]*Department of Physics, Hokkaido University, Sapporo 060-0810, Japan*
[4]*RIKEN Nishina Center, Wako, Saitama 351-0198, Japan*
[5]*Institute of Modern Physics, Fudan University, Shanghai 200433, China*

(Received 27 July 2022; accepted 1 November 2022; published 14 November 2022)

The α clustering in ^{10}Be and ^{12}Be has been studied within the framework of the real-time evolution method (REM). By using the effective interaction tuned to reproduce the charge radii and the threshold energies, we have evaluated the α reduced width amplitude (RWA) and spectroscopic factor (S factor) for the ground and excited states. With several improvements made in this work, comparing with our previous calculations, larger rates of clustering results are obtained for ^{10}Be and ^{12}Be with correct asymptotics at large distance.

DOI: 10.1103/PhysRevC.106.054313

I. INTRODUCTION

In nuclear physics, clustering phenomena have been intensively investigated by many experimental and theoretical studies [1–4]. One of the most important examples is the Hoyle state [5–12], which has a clustered structure composed of three α particles, and plays an essential role in the synthesis of carbon in the universe [13]. For decades, the clustering in light stable nuclei has been studied by various experimental methods such as resonant scattering, transfer reactions, and breakup reactions [14,15]. On the other hand, the clustering in neutron-rich nuclei is not known in as much detail as that in stable nuclei, due to limited experimental techniques [16,17].

Recently, the proton-induced α knockout reaction (p, $p\alpha$) was established as a quantitative measure of α-cluster formation at the nuclear surface [18–23]. The reaction was used to measure the α clustering in the Sn isotope chain [24], and revealed negative correlation between the α-cluster formation and the neutron-skin thickness [25]. This fascinating experiment opened a gate to explore the α clustering in the light neutron-rich nuclei. In fact, a (p, $p\alpha$) experiment is in preparation to measure the α clustering in the Be and C isotopes. Combined with the data obtained from breakup reactions, it will provide comprehensive information on how the clustering in the ground and excited states evolves as a function of neutron number. Therefore, an accurate microscopic calculation is highly desired for deeper understanding of the α clustering in light neutron-rich nuclei.

In our previous work, we adopted the antisymmetrized molecular dynamics (AMD) framework to evaluate α formation probability in Be and C isotopes [26,27]. The calculations showed the negative correlation between α clustering and neutron-skin thickness in the C isotopes, which is qualitatively consistent with what was observed in the Sn isotopes. However, from a quantitative point of view, those AMD results may underestimate the α formation probability for the following reasons. First, the Gogny D1S density functional in our previous study cannot describe light s- and p-shell nuclei accurately, because its parameters are optimized for medium- and heavy-mass nuclei [28]. In particular, it does not reproduce the α and ^{6}He decay threshold energies and radii of He isotopes, both of which strongly affect the cluster formation probability. Second, in our AMD+GCM (generator coordinate method) calculation, we used the quadrupole deformation parameter β as the generator coordinate. However, this choice does not span a model space large enough to describe various cluster motions in nuclei, in particular that at a large intercluster distance. In fact, it has been pointed out that an AMD+GCM calculation undershoots the α cluster formation probability of ^{48}Ti by an order of magnitude [29].

To overcome those defects, we perform alternative theoretical calculations with the following improvements. First, we adopt the Volkov No. 2 interaction [30] for the nucleon-nucleon interaction, which reproduces the radius of the α particle and the phase shift of the α-α scattering. For the spin-orbit interaction, we employed the G3RS interaction. We tuned the parameter sets of these interactions to reproduce the threshold energies. We also note that the combination of those interactions has been adopted in many microscopic calculations to discuss the energy spectrum of light nuclei [31,32]. Second, we employ the real-time evolution method (REM) to generate basis wave functions to describe various cluster motions. This method has successfully described the α clustering of Be and of C isotopes [33–35]. With these improvements, we obtained a more reliable cluster formation probability which has the correct asymptotics at a large distance. As we *a priori* assume the $\alpha + \alpha + xn$ cluster structure of ^{10}Be and ^{12}Be, this work will give the upper limit of α

*zhaoqing91@zjhu.edu.cn

cluster formation probability, whereas our previous study by AMD may give the lower limit.

This paper is organized as follows. In the next section, the theoretical framework of the generator coordinates method (GCM) with the real-time evolution method (REM) and the method to evaluate the reduced width amplitude (RWA) are briefly explained. In Sec. III, we present the numerical results and discuss the differences in the results between the AMD and the REM. The final section summarizes this work.

II. THEORETICAL FRAMEWORK

A. The Hamiltonian and the wave function

The Hamiltonian adopted in this study is given as

$$\hat{H} = \sum_{i=1}^{A} \hat{t}_i - \hat{T}_{c.m.} + \sum_{i<j}^{A} \hat{v}_N(\boldsymbol{r}_{ij}) + \sum_{i<j}^{A} \hat{v}_C(\boldsymbol{r}_{ij}) + \sum_{i<j}^{A} \hat{v}_{LS}(\boldsymbol{r}_{ij}), \tag{1}$$

where $\hat{t}_i$ and $\hat{T}_{c.m.}$ denote the kinetic energy operators of each nucleon and the center of mass, respectively. $\hat{v}_N$, $\hat{v}_C$, $\hat{v}_{LS}$ denote the effective nucleon-nucleon interaction, the Coulomb interaction, and the spin-orbit interaction, respectively.

In this work, we use the Volkov No. 2 interaction for the central nucleon-nucleon interaction [30], which is expressed as

$$\hat{v}_N(\boldsymbol{r}_{ij}) = (W - M\hat{P}^\sigma \hat{P}^\tau + B\hat{P}^\sigma - H\hat{P}^\tau) \times \left[V_1 \exp\left(-\boldsymbol{r}_{ij}^2/c_1^2\right) + V_2 \exp\left(-\boldsymbol{r}_{ij}^2/c_2^2\right)\right], \tag{2}$$

where W, M, B, and H denote the Wigner, Majorana, Bartlett, and Heisenberg exchanges, whose strengths are explained in the next section. The other parameters are, $V_1 = -60.65$ MeV, $V_2 = 61.14$ MeV, $c_1 = 1.80$ fm, and $c_2 = 1.01$ fm. For the spin-orbit interaction, we use the G3RS potential [36,37],

$$\hat{v}_{LS}(\boldsymbol{r}_{ij}) = V_{ls}\left(e^{-d_1 r_{ij}^2} - e^{-d_2 r_{ij}^2}\right)\hat{P}_{31}\hat{L}\cdot\hat{S}. \tag{3}$$

Here $\hat{P}_{31}$ projects the two-body system into a triplet odd state, which can be expressed as $\hat{P}_{31} = \frac{1+\hat{P}^\sigma}{2}\cdot\frac{1+\hat{P}^\tau}{2}$. The Gaussian range parameters d_1 and d_2 are set to 5.0 and 2.778 fm^{-2}, respectively.

We approximate the He and Be isotopes as being composed of α clusters plus valence nucleons. Thus, the wave functions of these isotopes are written as

$$\Phi(z_{\alpha_1}\ldots Z_1, Z_2\ldots) = \mathcal{A}\left\{\Phi_\alpha(z_{\alpha_1})\ldots\phi(Z_1)\phi(Z_2)\ldots\right\}, \tag{4}$$

where $\Phi_\alpha(z_\alpha)$ is the antisymmetrized wave function of the α cluster with $(0s)^4$ configuration oriented at z_α. $\phi(Z)$ are the single-neutron wave functions. The single-particle wave functions $\phi(\boldsymbol{r}, Z)$ are expressed in a Gaussian form multiplied by the spin-isospin part $\chi\tau$ as

$$\phi(\boldsymbol{r}, Z) = \left(\frac{2\nu}{\pi}\right)^{3/4}\exp\left[-\nu\left(\boldsymbol{r} - \frac{z}{\sqrt{\nu}}\right)^2 + \frac{1}{2}z^2\right]\chi\tau, \quad Z \equiv (z, a, b). \tag{5}$$

Here Z represents the time-dependent parameters of the wave function, which includes the three-dimensional coordinate z for the spatial part of the wave function as well as the spinors a and b for the spin part $\chi = a|\uparrow\rangle + b|\downarrow\rangle$. The isospin part is $\tau = \{\text{proton or neutron}\}$. The harmonic oscillator parameter is set to $b = \sqrt{1/(2\nu)} = 1.46$ fm for both the α cluster and neutron wave functions, which is same with that used in Refs. [31,38].

B. Real-time evolution method

We use the real-time evolution method (REM) [34,35] to generate the basis wave functions, which have various cluster configurations in the phase space. From the time-dependent variational principle,

$$\delta\int dt\,\frac{\left\langle\Phi(z_{\alpha_1},\ldots,Z_1,Z_2,\ldots)\right|i\hbar d/dt - \hat{H}\left|\Phi(z_{\alpha_1},\ldots,Z_1,Z_2,\ldots)\right\rangle}{\left\langle\Phi(z_{\alpha_1},\ldots,Z_1,Z_2,\ldots)\middle|\Phi(z_{\alpha_1},\ldots,Z_1,Z_2,\ldots)\right\rangle}. \tag{6}$$

We obtain the equation of the motion (EOM) for all the time-dependent parameters $Z(t)$ as

$$i\hbar\sum_{j=\alpha_1,1,2}\sum_{\sigma=x,y,z,a} C_{i\rho j\sigma}\frac{dZ_{j\sigma}}{dt} = \frac{\partial\mathcal{H}_{\rm int}}{\partial Z_{i\rho}^*}, \tag{7}$$

$$\mathcal{H}_{\rm int} \equiv \frac{\left\langle\Phi(z_{\alpha_1},\ldots,Z_1,Z_2,\ldots)\right|\hat{H}\left|\Phi(z_{\alpha_1},\ldots,Z_1,Z_2,\ldots)\right\rangle}{\left\langle\Phi(z_{\alpha_1},\ldots,Z_1,Z_2,\ldots)\middle|\Phi(z_{\alpha_1},\ldots,Z_1,Z_2,\ldots)\right\rangle}, \tag{8}$$

$$C_{i\rho j\sigma} \equiv \frac{\partial^2\ln\left\langle\Phi(z_{\alpha_1},\ldots,Z_1,Z_2,\ldots)\middle|\Phi(z_{\alpha_1},\ldots,Z_1,Z_2,\ldots)\right\rangle}{\partial Z_{i\rho}^*\partial Z_{j\sigma}}. \tag{9}$$

By solving this EOM starting from a certain wave function, a series of basis wave functions for the generator coordinate method (GCM) is obtained.

Under the framework of GCM, the basis wave functions with different parameters Z are superposed to describe the total wave function

$$\Psi_M^{J^\pi} = \int_0^{T_{\rm max}} dt\sum_{K=-J}^{J}\hat{P}_{MK}^{J^\pi} f_K(t)\Phi(z_{\alpha_1}(t),\ldots,Z_1(t),Z_2(t),\ldots), \tag{10}$$

where $\hat{P}^{J^\pi}_{MK}$ is the parity and the angular momentum projector. This integral can be approximately discretized as

$$\Psi^{J^\pi}_M = \sum_{i,K} \hat{P}^{J^\pi}_{MK} f_{i,K}(t)\Phi_i. \tag{11}$$

The corresponding coefficients $f_{i,K}$ and the eigenenergy E are obtained by solving the Hill-Wheeler equation.

C. α reduced width amplitude

To evaluate the degree of α clustering, we calculate the α reduced width amplitude (RWA) from the obtained wave functions, which is defined as the overlap amplitude between the A-body wave function of the mother nucleus Ψ and the reference state composed of clusters with mass numbers C_1 and C_2,

$$ay_l(a) = a\sqrt{\frac{A!}{(1+\delta_{C_1C_2})C_1!C_2!}}\left\langle \frac{\delta(r-a)}{r^2}\Psi_{C_1}\Psi_{C_2}Y_l(\hat{r})\middle|\Psi\right\rangle, \tag{12}$$

where Ψ_{C_1} and Ψ_{C_2} are the ground state wave functions of the two clusters. In Refs. [39,40], the approximated RWAs of ^{10}Be and ^{12}Be were calculated. In the current work, this equation is calculated by using the Laplace expansion method [41]. The α clustering may be evaluated by the α spectroscopic factor, which is defined as the squared integral of the RWA,

$$S_\alpha = \int_0^\infty r^2 dr\ y_l^2(r). \tag{13}$$

Note that S_α is not normalized to unity because of the anti-symmetrized effects between the clusters. In addition, we also introduce the root-mean-square radius of RWA,

$$R_{rwa} = \sqrt{\frac{\int_0^\infty r^4 dr, y_l^2(r)}{\int_0^\infty r^2 dr\, y_l^2(r)}}, \tag{14}$$

which is a measure of the average distance between clusters.

III. RESULTS

A. Structure properties of ^{10,12}Be and applied interaction parameters

For the calculation of ^{10}Be, we set the strengths of the central and spin-orbit interactions as $W = 0.4$, $M = 0.6$, $B = H = 0.125$, and $V_{ls} = 2000$ MeV. This parameter set has already been adopted in many calculations for this nucleus [31,32]. The obtained numerical results are denoted as "REM (set1)" in Table I, where the numerical results are compared with those obtained by the AMD calculation with the Gogny D1S interaction. The α-decay threshold energy is an important quantity for the discussion of the α-cluster formation. We see that the AMD fails to reproduce it, while the REM yields a consistent result with the experimental data. The charge radius is another important quantity to discuss the α formation probability. The AMD results overestimate the charge radii of light nuclei. The REM also overestimates them but is smaller than the AMD result. In short, the REM with the Volkov No. 2 interaction provides a better description of α threshold energy and the charge radius. We will discuss how these differences affect the RWA in the next subsection.

TABLE I. The numerical results of the 0^+ ground states of ^{10}Be, ^{6}He, and ^{4}He. "Expt.," "AMD," and "REM (set1)" denote the results from experimental data, AMD calculations, and REM calculations, respectively. R_c denotes the charge radius, which is calculated from the point proton radius. The experimental data of charge radius are from Ref. [45]. $\Delta E(\alpha)$ represents the threshold energy of ^{6}He + ^{4}He.

^{10}Be	Expt.	AMD	REM (set1)
$E(^6\text{He})$	−29.27 MeV	−33.04 MeV	−27.68 MeV
$E(^4\text{He})$	−28.30 MeV	−29.68 MeV	−27.57 MeV
$E(^{10}\text{Be})$	−64.98 MeV	−66.46 MeV	−62.46 MeV
$R_c(^{10}\text{Be})$	2.34 fm	2.62 fm	2.55 fm
$\Delta E(\alpha)$	−7.41 MeV	−3.75 MeV	−7.21 MeV

It has been known that the ^{8}He + ^{4}He and ^{6}He + ^{6}He configurations and even the ^{7}He + ^{5}He configuration play important roles in the low-lying states of ^{12}Be [2,17,42,43]. The ground state of ^{12}Be is dominated by the configuration with the breaking of the $N = 8$ magic number [32,42,44], and the 0^+_2 state has $N = 8$ closed shell structure. The numerical results are shown as "REM (set1)" in Table II. We found that REM does not reproduce many properties of ^{12}Be if we apply the same interaction parameters as ^{10}Be.Furthermore, the order of α+^{8}He and ^{6}He + ^{6}He channels, denoted by $\Delta E(\alpha)$ and $\Delta E(^6\text{He})$, is inverted from the experimental data. We also find that the breaking of the magic number in the ground state cannot be reproduced from the RWA results. Therefore, we slightly changed the Majorana parameters and the strength of the spin-orbit interaction to be $M = 0.58$ ($W = 1 - M$) and $V_{ls} = 2800$ to reproduce the following properties: the breaking of the magic number in the ground state, the α+^{8}He and ^{6}He + ^{6}He threshold energies, and the excitation energy of the 0^+_2 state. The results obtained by the fitted interaction are denoted by "REM (set2)" in Table II. This guarantees consistency with the observed data.

TABLE II. The numerical results of the 0^+ ground states of ^{12}Be, ^{8}He, and ^{4}He. The meanings of the symbols are the same as in the previous table. The experimental data of charge radius are from Ref. [46]. $E_x(0^+)$ denotes the excitation energy of the first excited 0^+ state. $\Delta E(\alpha)$ and $\Delta E(^6\text{He})$ represent the threshold energies of ^{8}He + ^{4}He and ^{6}He + ^{6}He, respectively.

^{12}Be	Expt.	AMD	REM (set1)	REM (set2)
$E(^{12}\text{Be})$	−68.65 MeV	−68.70 MeV	−60.89 MeV	−69.80 MeV
$E_x(0^+)$	2.25 MeV	1.96 MeV	5.54 MeV	2.76 MeV
$R_c(^{12}\text{Be})$	2.50 fm	2.82 fm	2.47 fm	2.45 fm
$E(^8\text{He})$	−31.40 MeV	−33.65 MeV	−26.18 MeV	−35.64 MeV
$E(^6\text{He})$	−29.27 MeV	−33.04 MeV	−27.68 MeV	−29.85 MeV
$E(^4\text{He})$	−28.30 MeV	−29.68 MeV	−27.57 MeV	−27.57 MeV
$\Delta E(\alpha)$	−8.96 MeV	−5.37 MeV	−7.13 MeV	−6.59 MeV
$\Delta E(^6\text{He})$	−10.11 MeV	−2.63 MeV	−5.53 MeV	−10.11 MeV

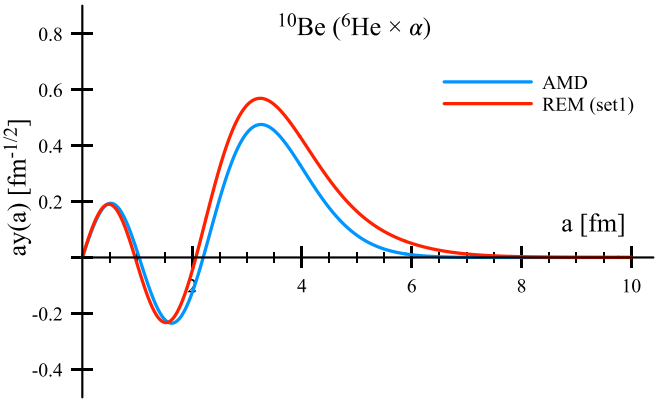

FIG. 1. The calculated RWA of the ground state of ^{10}Be in the ^{6}He + ^{4}He channel. All the nuclei are in the ground state.

B. RWA and Whittaker function

Before we discuss the RWA, we recall the structure of ^{10}Be and ^{12}Be, which have been fully investigated by many kinds of microscopic models [47–53]. Two valence neutrons of ^{10}Be occupy the p shell, whereas two of four valence neutrons in ^{12}Be are promoted to the sd shell across the $N = 8$ shell gap. We then compare the RWA calculation results to see the similarities and differences in the α cluster formation probability obtained by AMD and REM frameworks. Figure 1 shows the RWA of the ground state of ^{10}Be for the ^{6}He + ^{4}He channel. It shows that the REM provides a much larger amplitude than the AMD calculation at the peak region, which indicates the larger possibility of α formation in ^{10}Be. This is due to the α cluster assumption in the REM wave function, while the AMD does not assume it. Therefore, the current REM result provides the upper limit of clustering. In addition to the difference in the amplitude, it can be found that the positions of the nodes of RWA from REM are shifted slightly to the inner part compared with the AMD calculations, which indicates a shorter spatial distribution of the α cluster. This is because REM gives a smaller radius of the ^{10}Be ground state. Thus, REM yields a more enhanced but narrower distribution of the α cluster.

An advantage of REM over AMD is that it can describe the correct asymptotics of RWA. As explained in the Appendix, the RWA should be identical to the Whittaker function at a large distance. We compare the logarithmic derivatives of the RWA and the Whittaker function in Fig. 2. We can see that the RWA calculated from the AMD is inconsistent with the Whittaker function, whereas REM yields the correct asymptotics. From this result, we can easily obtain the asymptotic normalization constant (ANC), which is calculated as 5.3.

Unlike ^{10}Be, the discussion of ^{12}Be is complicated because of its more exotic structure. In Fig. 3, we show the RWA of the ground state of ^{12}Be calculated by using the original and modified interaction parameters. First, we note that the number of nodes of RWA is different depending on the choice of the interaction parameter sets. This is due to the difference in the structure of the ground state. In the case of the original parameter set, all valence neutrons occupy the p shell in contradiction to the experimental fact. On the other hand, in the

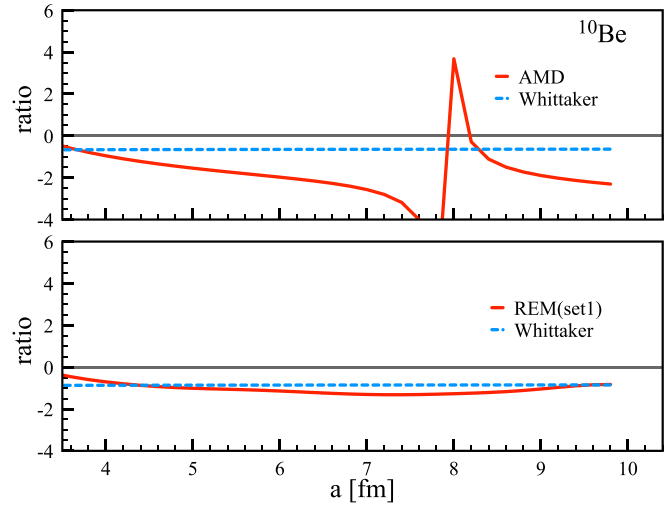

FIG. 2. The comparison of results between the calculated RWA and the Whittaker function for ^{10}Be beyond 3.5 fm. The vertical axis shows the ratio between the derivatives of the functions as in Eq. (A6).

case of the modified parameter set, the ground state is dominated by the $2\hbar\omega$ configuration, in which two valence neutrons are excited into the sd shell across the $N = 8$ shell gap. As a result, the RWA obtained by using the modified parameter set has an additional node. Second, we again see a larger amplitude at the peak value in the modified parameter set calculation than the AMD result, which can also be attributed to the cluster assumption node in the REM calculation. We also see that the RWA from the AMD calculation is much more spread out than the REM (set2) calculation. This is because of the much-overestimated radii of the AMD results.

The comparison between the RWA and the Whittaker function is shown in Fig. 4. The deviations from the Whittaker function are found for both of the AMD and REM (set2) calculations. This result may be explained as follows. The Whittaker function assumes a two-body system. However, as already been discussed in many papers [42,54], the ground state of ^{12}Be is an admixture of the ^{8}He + ^{4}He, ^{6}He + ^{6}He, and ^{5}He + ^{7}He channels. This fact can also be seen in Fig. 5,

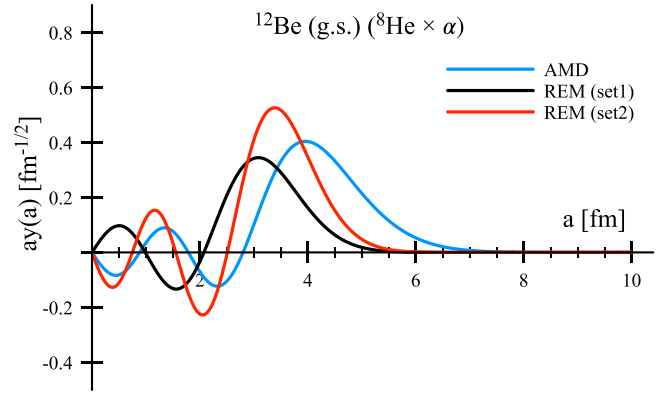

FIG. 3. The calculated RWA of ^{12}Be in the ^{8}He + ^{4}He channel. All the nuclei are in the ground state.

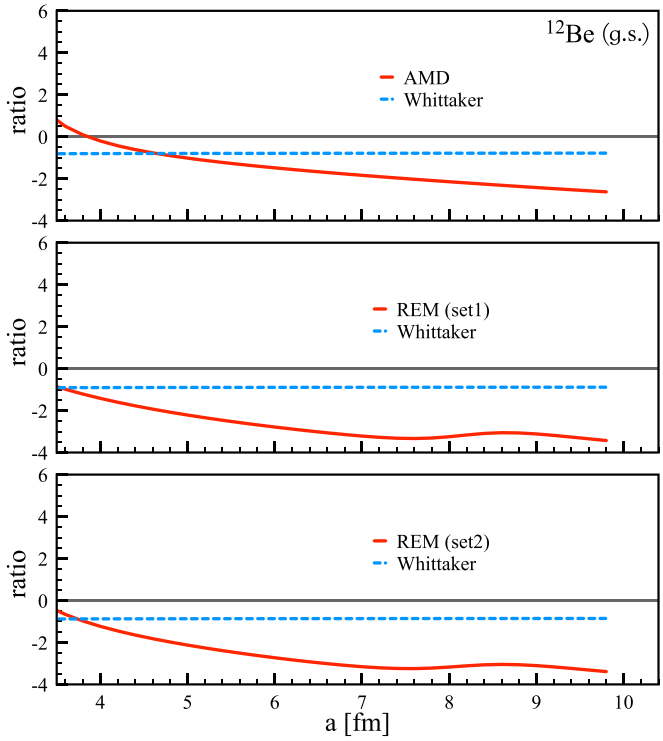

FIG. 4. The comparison results between the calculated RWA and the Whittaker function for ^{12}Be. The vertical axis shows the ratio between the derivatives of the functions as in Eq. (A6).

where the amplitudes of RWAs for ^{12}Be are compared between ^{6}He + ^{6}He and ^{8}He + ^{4}He channels. Therefore, the ground state of ^{12}Be cannot be simply treated as a two-body system, which causes a departure from the Whittaker function.

In addition to the limitation of the two-body system assumption, the requirement that the cluster is only affected by the Coulomb interaction may also be violated by the RWA to cause the departure from the Whittaker function. As already shown in Table III, the rms radii of point neutrons are much larger than those of point protons for ^{12}Be, especially in the REM calculations. It suggests that the formed cluster in ^{12}Be may be surrounded by valence neutrons even in the outer region of the nucleus so that the cluster still feels residual nuclear force. This residual nuclear force from the neutrons also leads to the departure from the Whittaker function. Another cause can be found from the RWA results of the 0^+_2 state for ^{12}Be shown in Fig. 6. It shows that the middle region of ^{12}Be is dominated by the ^{6}He + ^{6}He channel while the outside region is dominated by the ^{8}He + ^{4}He channel, which should satisfy the assumption of a two-body system. However, the amplitudes of RWA are only visible within about 5 fm, where the nuclear force cannot be neglected. This narrow distribution of RWA also causes the departure from the Whittaker function as shown in Fig. 7.

TABLE III. The calculated rms radii of point neutron and proton distributions. All the units are in fm.

	^{10}Be(g.s.)		^{12}Be(g.s.)		^{12}Be(0^+_2)	
	AMD	REM	AMD	REM (set2)	AMD	REM (set2)
r_n	2.50	2.53	2.91	2.50	2.67	2.52
r_p	2.43	2.35	2.63	2.23	2.52	2.21

Finally, we show the α spectroscopic factors and the rms radii of RWA in Table IV.It explicitly shows that the AMD result may provide a lower limit of the α clustering in the Be isotopes, while the REM procedure with the Volkov No 2 interaction may provide the upper limit. Both calculations show the suppression of clustering with increasing neutron number, especially in the REM calculation, which satisfies the discussion on the effect of the neutron-skin thickness in Ref. [24] and our previous work [26]. In addition, AMD suggests counterintuitive enhanced rms radii of RWA, which describes a broader average region of α clustering even with the suppression by the neutron skin thickness. However, the REM calculations, in contrast, can show a slight suppression of radii. These results again suggest that the REM procedure with the Volkov No. 2 interaction under the cluster model could be more appropriate for the description of the α clustering in the light nuclei.

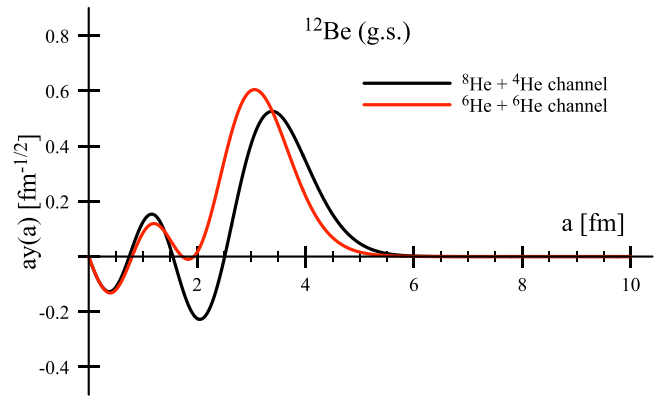

FIG. 5. The comparison of calculated RWA for ^{12}Be between the ^{8}He + ^{4}He channel and the ^{6}He + ^{6}He channel. All the nuclei are in the ground state.

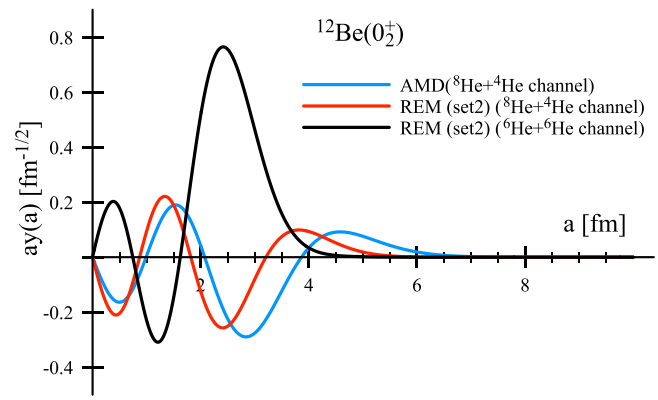

FIG. 6. The calculated RWA of the second 0^+ state of ^{12}Be in the ^{8}He + ^{4}He and ^{6}He + ^{6}He channels. All the nuclei are in the ground state.

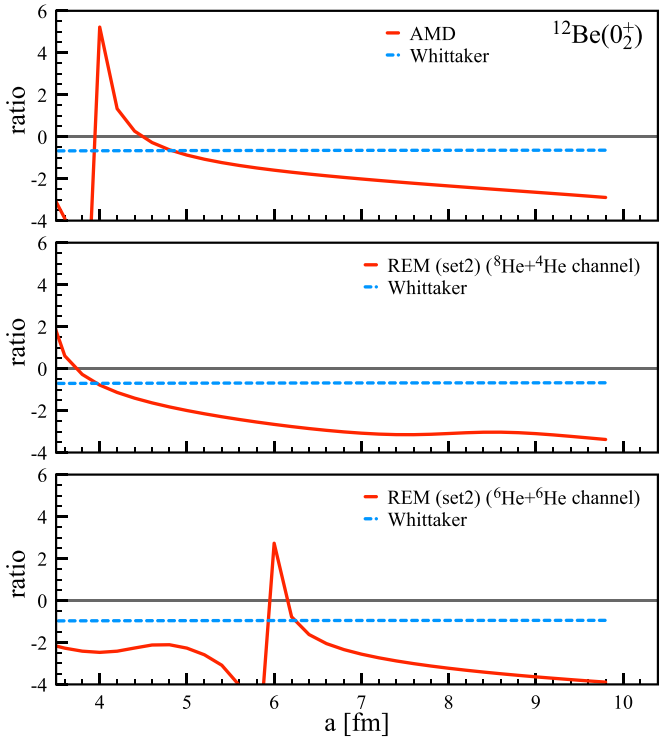

FIG. 7. The comparison results between the calculated RWA and the Whittaker function for ^{12}Be. The vertical axis shows the ratio between the derivatives of the functions as in Eq. (A6).

IV. SUMMARY

The RWAs of ^{10}Be and ^{12}Be were calculated with the REM procedure, where the cluster model and the Volkov No. 2 interaction are adopted. Compared with the results from previous AMD calculations, the new results can reproduce the charge radii and the threshold energies. These quantities could be more important for the description of α clustering. The RWA results from these frameworks show that the REM procedure may provide the upper limit of α clustering, while the AMD gives the lower limit. Besides, the suppression in rms radius of RWA by the neutron skin thickness can be correctly obtained by the REM calculations.

The Whittaker function is expected to be an important criterion for testing the calculation of cluster formation. The comparison with the Whittaker function shows that the current REM result of ^{10}Be provides the correct asymptotics at large distance, which indicates more reliable description on the α cluster formation.

TABLE IV. The calculated S factor and rms radius of RWA.

	^{10}Be		^{12}Be	
	AMD	REM	AMD	REM (set2)
S_α	0.35	0.54	0.24	0.33
R_{rwa}	3.23 fm	3.41 fm	4.07 fm	3.36 fm

For the calculation of ^{12}Be, the breaking of the $N = 8$ magic number is reproduced by slightly modifying the parameters of the interaction. The RWA results of ^{12}Be suggest the mixing of the ^{8}He + ^{4}He channel and ^{6}He + ^{6}He channel in the ground state. This complex structure causes the departure from the Whittaker function. In addition to this, the narrow distribution of the RWA and the influence of the valence neutrons may also affect the asymptotics of RWA. The behavior of RWA in nuclei with exotic cluster structures or neutron skin will be further investigated in our future works.

ACKNOWLEDGMENTS

The authors thank Dr. Z. H. Yang and Dr. K. Ogata for fruitful discussions. This work was supported by National Natural Science Foundation of China (Grants No. 12147219, No. 11961141003, No. 12275081, and No. 12275082), and JSPS KAKENHI (Grants No. 19K03859, No. 21H00113 and No. 22H01214). Numerical calculations were performed in the server at the Theoretical Nuclear Physics Laboratory, Hokkaido University, and the Cluster-Computing Center of School of Science (C3S2) at Huzhou University.

APPENDIX: WHITTAKER FUNCTION

The RWA can be treated as the wave function of the α cluster in the mother nucleus. Therefore, it should be the solution of the time-independent Schrödinger equation:

$$-\frac{\hbar^2}{2m}\nabla^2\psi + V(r)\psi = E\psi. \tag{A1}$$

In the case of two-body system, r is the distance between two particles and m is the reduced mass. $V(r)$ represents the potential between two particles and the eigenvalue E will be the threshold energy between them.

Considering the situation when the formed cluster is too far away from the residue nucleus, only the Coulomb potential is present, then the solutions of Eq. (A1) are the Whittaker functions [55,56]:

$$u_1 = M_{-\eta,l+\frac{1}{2}}(2kr)$$
$$u_2 = W_{-\eta,l+\frac{1}{2}}(2kr) \tag{A2}$$

where l is relative angular momentum between two particles and other parameters are summarised as

reduced mass: $m = m_1 m_2/(m_1 + m_2)$

wave number: $k = \sqrt{-2mE/\hbar^2}$

$\times$ dimensionless Sommerfeld parameter:

$$\eta = Z_1 Z_2 e^2 m/4\pi\epsilon_0\hbar^2 k. \tag{A3}$$

Among these two solutions, we only adopt the Whittaker W function for the physical meaning.

In this sense, if the RWA calculated from a framework is accurate enough, it should be identical to the Whittaker

function starting from a large distance a with an normalization factor C as

$$ry_l(r) = CW(r) \text{ for } r > a. \tag{A4}$$

This factor C is called asymptotic normalization constant (ANC), which is of importance for the study of the astrophysical reactions [57–59]. In addition, if C is really a constant in the calculation, the derivative of Eq. (A4) should still hold as

$$[ry_l(r)]' = CW'(r) \qquad \text{for } r > a. \tag{A5}$$

Therefore, by comparing the ratios between Eqs. (A4) and (A5),

$$\frac{[ry_l(r)]'}{ry_l(r)}, \qquad \frac{W'(r)}{W(r)}, \tag{A6}$$

the existence of the constant C can be confirmed if these two ratios are identical. The comparison between RWA and the Whittaker equation can be treated as an important criterion of the accuracy of the calculation. In this work, we compare the RWA obtained from AMD and REM calculations with the Whittaker function to discuss the model dependence of the description of cluster formation.

[1] P. Descouvemont, Phys. Rev. C **39**, 1557 (1989).
[2] W. von Oertzen, Phys. Rev. **432**, 43 (2006).
[3] H. Horiuchi, Nucl. Phys. A **522**, 257 (1991).
[4] Y. Fujiwara, H. Horiuchi, K. Ikeda, M. Kamimura, K. Katō, Y. Suzuki, and E. Uegaki, Prog. Theor. Phys. Suppl. **68**, 29 (1980).
[5] F. Hoyle, Astrophys. J. Suppl. Ser. **1**, 121 (1953).
[6] C. W. Cook, W. A. Fowler, C. C. Lauritsen, and T. Lauritsen, Phys. Rev. **107**, 508 (1957).
[7] E. Uegaki, S. Okabe, Y. Abe, and H. Tanaka, Prog. Theor. Phys. **57**, 1262 (1977).
[8] E. Uegaki, Y. Abe, S. Okabe, and H. Tanaka, Prog. Theor. Phys. **59**, 1031 (1978).
[9] M. Kamimura, Nucl. Phys. A **351**, 456 (1981).
[10] A. Tohsaki, H. Horiuchi, P. Schuck, and G. Röpke, Phys. Rev. Lett. **87**, 192501 (2001).
[11] Y. Kanada-En'yo, Phys. Rev. Lett. **81**, 5291 (1998).
[12] M. Chernykh, H. Feldmeier, T. Neff, P. von Neumann-Cosel, and A. Richter, Phys. Rev. Lett. **98**, 032501 (2007).
[13] H. O. U. Fynbo *et al.*, Nature (London) **433**, 136 (2005).
[14] Y. Liu, Y. L. Ye, J. L. Lou, X. F. Yang, T. Baba, M. Kimura *et al.*, Phys. Rev. Lett. **124**, 192501 (2020).
[15] W. H. Ma, D. Patel, Y. Y. Yang *et al.*, Phys. Rev. C **103**, L061302 (2021).
[16] Y. Kanada-En'yo and H. Horiuchi, Phys. Rev. C **52**, 647 (1995).
[17] M. Kimura, T. Suhara, and Y. Kanada-En'yo, Eur. Phys. J. A **52**, 373 (2016).
[18] K. Yoshida, K. Minomo, and K. Ogata, Phys. Rev. C **94**, 044604 (2016).
[19] T. Wakasa, K. Ogata, and T. Noro, Prog. Part. Nucl. Phys. **96**, 32 (2017).
[20] K. Yoshida, K. Ogata, and Y. Kanada-En'yo, Phys. Rev. C **98**, 024614 (2018).
[21] K. Yoshida, Y. Chiba, M. Kimura, Y. Taniguchi, Y. Kanada-En'yo, and K. Ogata, Phys. Rev. C **100**, 044601 (2019).
[22] K. Yoshida and J. Tanaka, Phys. Rev. C **106**, 014621 (2022).
[23] T. A. Carey, P. G. Roos, N. S. Chant, A. Nadasen, and H. L. Chen, Phys. Rev. C **23**, 576(R) (1981).
[24] J. Tanaka, Z. Yang, S. Typel *et al.*, Science **371**, 260 (2021).
[25] S. Typel, Phys. Rev. C **89**, 064321 (2014).
[26] Q. Zhao, Y. Suzuki, J. He *et al.*, Eur. Phys. J. A **57**, 157 (2021).
[27] J. He, Master's thesis, Hokkaido University, 2021 (unpublished).
[28] J. Berger, M. Girod, and D. Gogny, Comput. Phys. Commun. **63**, 365 (1991).
[29] Y. Taniguchi, K. Yoshida, Y. Chiba *et al.*, Phys. Rev. C **103**, L031305 (2021).
[30] A. Volkov, Nucl. Phys. **74**, 33 (1965).
[31] N. Itagaki, A. Kobayakawa, and S. Aoyama, Phys. Rev. C **68**, 054302 (2003).
[32] Y. Kanada-En'yo, M. Kimura, and A. Ono, Prog. Theor. Exp. Phys. **2012**, 01A202 (2012).
[33] R. Imai, T. Tada, and M. Kimura, Phys. Rev. C **99**, 064327 (2019).
[34] B. Zhou, M. Kimura, Q. Zhao, and S. Shin, Eur. Phys. J. A **56**, 298 (2020).
[35] Q. Zhao, B. Zhou, M. Kimura *et al.*, Eur. Phys. J. A **58**, 25 (2022).
[36] R. Tamagaki, Prog. Theor. Phys. **39**, 91 (1968).
[37] N. Yamaguchi, T. Kasahara, S. Nagata, and Y. Akaishi, Prog. Theor. Phys. **62**, 1018 (1979).
[38] T. Furumoto, T. Suhara, and N. Itagaki, Phys. Rev. C **97**, 044602 (2018).
[39] M. Lyu, K. Yoshida, Y. Kanada-En'yo, and K. Ogata, Phys. Rev. C **97**, 044612 (2018).
[40] M. Lyu, K. Yoshida, Y. Kanada-En'yo, and K. Ogata, Phys. Rev. C **99**, 064610 (2019).
[41] Y. Chiba and M. Kimura, Prog. Theor. Exp. Phys. **2017**, 053D01 (2017).
[42] M. Ito, N. Itagaki, and K. Ikeda, Phys. Rev. C **85**, 014302 (2012).
[43] M. Ito, K. Kato, and K. Ikeda, Phys. Lett. B **588**, 43 (2004).
[44] S. Shimoura *et al.*, Phys. Lett. B **654**, 87 (2007).
[45] M. Žáková, Z. Andjelkovic *et al.*, J. Phys. G: Nucl. Part. Phys. **37**, 055107 (2010).
[46] A. Krieger, K. Blaum, M. L. Bissell, N. Frömmgen, Ch. Geppert, M. Hammen *et al.*, Phys. Rev. Lett. **108**, 142501 (2012).
[47] F. Kobayashi and Y. Kanada-En'yo, Phys. Rev. C **86**, 064303 (2012).
[48] T. Neff, H. Feldmeier, and R. Roth, Nucl. Phys. A **752**, 321 (2005).
[49] P. Descouvemont and D. Baye, Phys. Lett. B **505**, 71 (2001).
[50] M. Ito, N. Itagaki, H. Sakurai, and K. Ikeda, Phys. Rev. Lett. **100**, 182502 (2008).
[51] H. T. Fortune and R. Sherr, Phys. Rev. C **83**, 044313 (2011).
[52] C. Romero-Redondo, E. Garrido, D. V. Fedorov, and A. S. Jensen, Phys. Rev. C **77**, 054313 (2008).

[53] T. Neff and H. Feldmeier, Eur. Phys. J.: Spec. Top. **156**, 69 (2008).
[54] Y. Kanada-En'yo, Phys. Rev. C **66**, 011303(R) (2002).
[55] P. Descouvemont and D. Baye, Rep. Prog. Phys. **73**, 036301 (2010).
[56] Carl R. Brune, Phys. Rev. C **102**, 034328 (2020).
[57] A. M. Mukhamedzhanov and R. E. Tribble, Phys. Rev. C **59**, 3418 (1999).
[58] N. K. Timofeyuk, R. C. Johnson, and A. M. Mukhamedzhanov, Phys. Rev. Lett. **91**, 232501 (2003).
[59] M. Freer, J. C. Angelique, L. Axelsson, B. Benoit, U. Bergmann, W. N. Catford *et al.*, Phys. Rev. C **63**, 034301 (2001).